Bioorganic & Medicinal Chemistry Letters 22 (2012) 6596–6601

Contents lists available at SciVerse ScienceDirect

Bioorganic & Medicinal Chemistry Letters

journal homepage: www.elsevier.com/locate/bmcl

Identification of novel 3,5-diarylpyrazoline derivatives containing salicylamide moiety as potential anti-melanoma agents

Qing-Shan Li [a,†], Xian-Hai Lv [b,†], Yan-Bin Zhang [a], Jing-Jun Dong [a], Wen-Ping Zhou [a], Yang Yang [a], Hai-Liang Zhu [a,*]

[a] State Key Laboratory of Pharmaceutical Biotechnology, Nanjing University, Nanjing 210093, PR China
[b] College of Science, Anhui Agricultural University, Hefei 230036, PR China

ARTICLE INFO

Article history:
Received 18 June 2012
Revised 17 August 2012
Accepted 1 September 2012
Available online 10 September 2012

Keywords:
BRAF
Inhibitors
Melanoma
Mutant
Virtual screening
3D-QSAR

ABSTRACT

There is an accumulating body of experimental evidences validating oncogenic $BRAF^{V600E}$ as a therapeutic target and offering opportunities for anti-melanoma drug development. Encouraged by the positive results of pyrazole derivatives as $BRAF^{V600E}$ inhibitors, we sought to design diverse novel potential $BRAF^{V600E}$ inhibitors as antitumor agents based on pyrazole skeleton. In silico and in vitro screening of our designed pyrazole derivatives has identified **Hit 1** as $BRAF^{V600E}$ inhibitor. Based on its structure and through further structure modification, compound **25**, which exhibited the most potent inhibitory activity with an IC_{50} value of 0.16 μM for $BRAF^{V600E}$ and GI_{50} value of 0.24 μM for mutant BRAF-dependent melanoma cells, was obtained. The 3D-QSAR models and the molecular docking simulation were introduced to analyze the structure–activity relationship.

The RAS-RAF-MEK-ERK (MAP kinases) cascade plays a key role in cellular growth, proliferation, and differentiation in response to many different external stimuli.[1,2] MAP kinases are regulated by phosphorylation cascades whereby activation of an upstream kinase leads to phosphorylation of a downstream substrate which itself has protein-kinase activity.[3,4] The RAS proteins are membrane-bound small G-protein, whereas RAF, MEK, and ERK are cytosolic protein-kinases that compose a sequential signaling cascade. Under normal circumstances, RAF is activated in a RAS small G-protein dependent manner. Then activated RAF activates (phosphorylates) MEK, which in turn activates a third protein-kinase called ERK. ERK phosphorylates transcription factors such as ELK-1, regulating gene expression and controlling how cells respond to extracellular signals.[5,6]

Cancers arise owing to the accumulation of mutations in critical genes that alter normal programs of cell proliferation, differentiation and death.[7] Mutations of RAF kinase were frequently found in cancer cells, results in it being the most studied drug target in this cascade. The RAF protein-kinase family consists of three isoforms named ARAF, c-RAF-1, and BRAF. The importance of BRAF activation was highlighted by more recent studies that showed that it is mutated approximately in 7% of human cancer, most notably in ovarian (~35%), thyroid (~30%), and colorectal (~10%) cancers, particularly in melanoma (50–70%).[8,9] The most common BRAF mutation in melanoma is the substitution of a valine for glutamic acid at position 600 (termed $BRAF^{V600E}$), resulting in a protein that has 500-fold elevated protein-kinase activity compared to the wild-type. $BRAF^{V600E}$ stimulates sustained and constitutive activation of the ERK pathway, inducing uncontrolled cell proliferation, increased cell survival, and tumor progression.[10,11] Inhibition of mutant BRAF signaling, through either direct inhibition of the enzyme or inhibition of MEK, has been demonstrated preclinical applications for inhibit melanoma development.[12,13] Recently, treatment of BRAF mutant melanoma patients with a selective BRAF inhibitor has resulted in antitumor activity,[14,15] These findings strongly implicate the BRAF protein-kinase as an important target for the development of small molecule inhibitors in the treatment of human melanoma.

Many pyrazole derivatives are acknowledged to possess a wide range of bioactivities,[16–18] and such pyrazole core has increasingly attracted the attention of synthetic chemists. Some small chemical molecules containing pyrazole skeleton have been identified as selective inhibitors of $BRAF^{V600E}$ and exhibited potent anti-cancer activities.[19,20] Encouraged by the positive results of previous research, we sought to design diverse novel potential $BRAF^{V600E}$ inhibitors for anti-melanoma agents based on pyrazole skeleton.

Abbreviations: BRAF, V-RAF murine sarcoma viral oncogene homologue B1; pERK, phosphorylated extracellular regulated kinase; $BRAF^{V600E}$, V600E mutant BRAF; $BRAF^{WT}$, BRAF wild-type; IC_{50}, half maximal inhibitory concentration; GI_{50}, the concentration that causes 50% growth inhibition; 3D-QSAR, Quantitative Structure–Activity Relationship.

* Corresponding author. Tel./fax: +86 25 83592672.
E-mail address: zhuhl@nju.edu.cn (H.-L. Zhu).

† Both authors contributed equally to the work

0960-894X/$ - see front matter © 2012 Elsevier Ltd. All rights reserved.
http://dx.doi.org/10.1016/j.bmcl.2012.09.004

Table 1
Initially positive results of virtual and protein-kinase inhibitory activities screening

Compound	Structure	Binding energies kcal/mol	$BRAF^{V600E}$ IC_{50}, μM
Hit 1	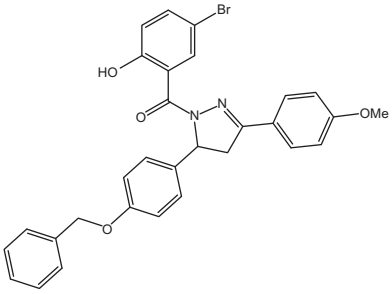	−20.97	7.22 ± 0.59
Hit 2	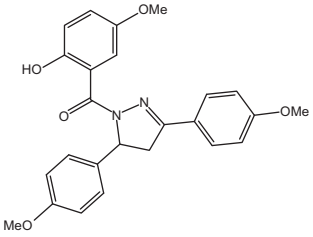	−17.66	8.38 ± 0.44

Result values are shown as mean values of three independent determinations.

For this purpose, we have designed more than 300 compounds based on pyrazole skeleton, including amide, (thio)urea, Schiff bases, chalcone, salicylamide, amine, thiazole and other derivatives of pyrazole. Virtual screening program and in vitro protein-kinase inhibitory activities evaluation were introduced to initial screening these candidate compounds.

In the virtual screening procedure, the docking program CDOCKER (Discovery Studio 3.1, Accelrys, Inc., San Diego, CA)[21,22] was used as the in silico screening tool. The $BRAF^{V600E}$/**SB-590885** crystal structure with the inhibitor removed from the coordinates (PDB ID: 2FB8)[23] was used as a receptor for compound binding. Residues within a distance of 10 Å around the BRAF inhibitor **SB-590885** were isolated for the construction of a grid for docking simulation. This grid was large enough to include every residue of the BRAF kinase ATP-binding pocket.[19] After screening our designed pyrazole derivatives, six initially candidate compounds with the lowest binding energies were selected for protein-kinase inhibitory activity screening. Two candidate compounds (**Hit 1** and **Hit 2**) which displayed the lowest IC_{50} $BRAF^{V600E}$ values were chosen for further study, and their structures, binding energies, $BRAF^{V600E}$ inhibitory activities were summarized in Table 1. Both **Hit 1** and **Hit 2** own pyrazoline salicylamide skeleton, so we focus on the structure and activity optimization of pyrazoline salicylamide derivatives in this study.

To take more directly insight into the binding mode of pyrazoline salicylamide derivatives and mutant BRAF, the binding model of (5-(4-(benzyloxy)phenyl)-3-(4-methoxyphenyl)-4,5-dihydro-1*H*-pyrazol-1-yl)(5-bromo-2-hydroxyphenyl)meth-anone (**Hit 1**) with BRAF structure are shown in Figure 1a and b. Visual inspection of the pose of **Hit 1** into BRAF binding site revealed that this candidate BRAF inhibitor was tightly embedded into the ATP binding pocket. The model suggests that extensive hydrophobic interactions are formed between **Hit 1** and residues Val 471, Ala 481, Lys 483, Leu 514, Ile 527, Thr 529, Phe 583 and Asp 594 of the ATP-binding pocket of BRAF kinase. Furthermore, a more optimal H-bond interaction was formed between its methoxyl group and the carbonyl group of Ser 535. Also, the phenolic hydroxyl group of **Hit 1** forms hydrogen bond with Ser 465. Compared with the binding mode of **SB-590885** (Fig. 1a), they both have good shape complementarity with ATP-binding pocket of BRAF, and their aromatic side chain were deeply embedded into the pocket. However, different interactions with amino acid residues in binding site were contributed to their combination with BRAF. For **SB-590885** (Fig. 1c), in addition to H-bonds formed with Glu 501 and Cys 532, π–π interaction was found between its aromatic imidazole ring and Phe 583. This additional π interaction of **SB-590885** possibly results in its orientation and conformation was different from that of **Hit 1** in BRAF.

On the basis of the positive results obtained with **Hit 1** and **Hit 2**, the 3,5-diarylpyrazoline skeleton could serve as a promising scaffold for developing new kinase inhibitors of V600E mutant BRAF. In order to obtain more pharmacophore understandings and carry on further rational structure optimization, various substituents were introduced to the aromatic systems of 3,5-diarylpyrazoline salicylamide. From the binding model, both the methoxyl and phenolic hydroxyl groups of candidate compound were beneficial for its binding affinity with mutant BRAF. So these two substituents were retained in the structure, and then several substituents were introduced into the ring A and ring B of pyrazoline salicylamide skeleton. The synthesis of twenty pyrazoline derivatives were synthesized in three steps, the synthesis followed the general pathway outlined in Scheme 1. The pyrazoline core (**5–8**) was synthesized via a two-step process in good yields: 1) aldol condensation between an appropriately substituted benzaldehyde and 4'-Methoxyacetophenone; 2) followed by pyrazoline formation by addition of hydrazine hydrate. Target pyrazole salicylamide derivatives **9–28** were synthesized by coupling appropriate substituted salicylic acid with equimolar quantities of **5–8**, using 1-ethyl-3-(3-dimethylaminopropyl) carbodiimide hydrochloride (EDC·HCl) and 1-hydroxybenzotriazole anhydrous (HOBt) as condensing agent. Analytical and spectroscopic data of all compounds were reported in **part 1** of Supplementary data, and were in full accordance with their depicted structures.

The biological activities (the data are summarized in Table 2) of these novel 3,5-diarylpyrazoline derivatives were determined using two assays: (1) the $BRAF^{V600E}$ inhibitory activities of these synthesized compounds were determined as their ability to inhibit BRAF mediated MEK phosphorylation (IC_{50} $BRAF^{V600E}$); (2) the determination of the growth inhibition in WM266.4 human melanoma cells expressing V600E mutant BRAF with MTT assay (GI_{50}

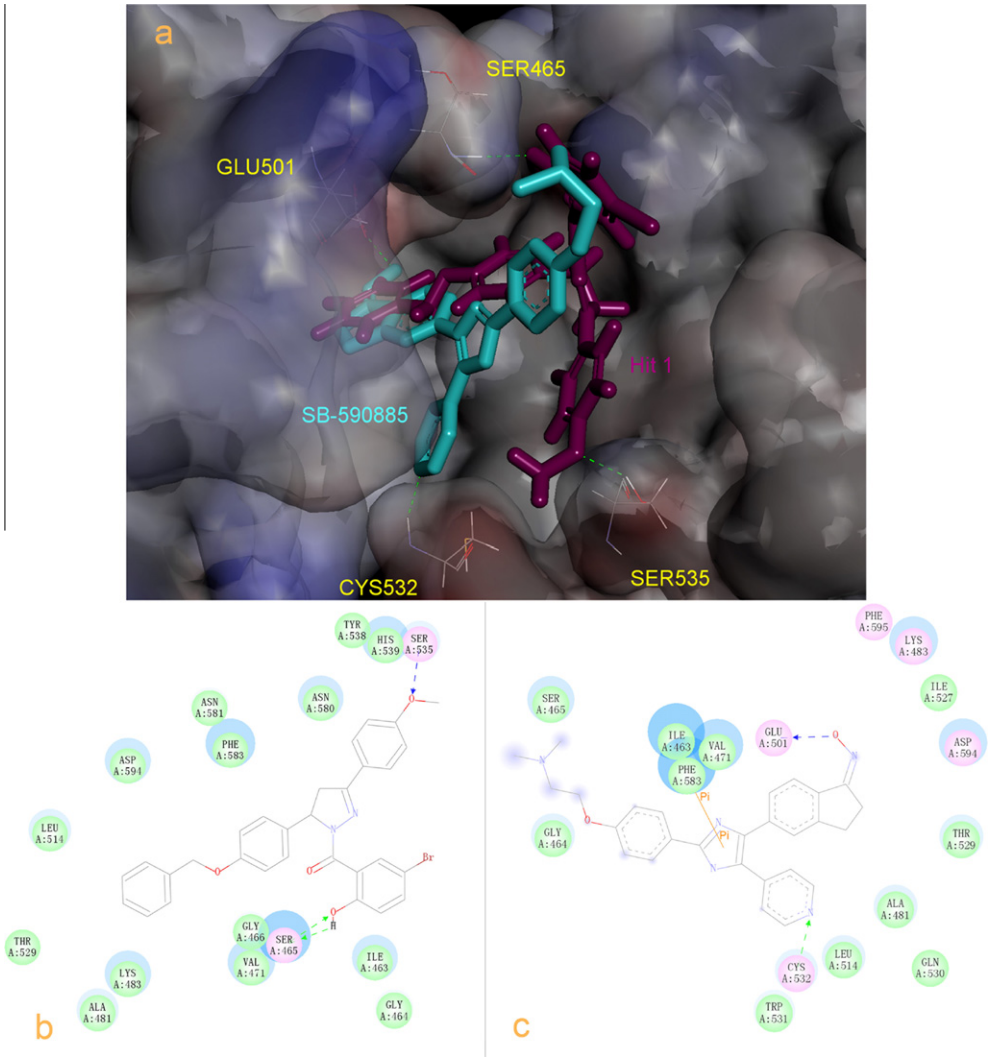

Figure 1. (a). Binding model of **Hit 1** (purple) and **SB-590885** (blue) in the active site of the $BRAF^{V600E}$ protein-kinase. The H-bond is displayed as dashed line. (b). and (c). 2D projection drawing of **Hit 1** and **SB-590885** docked into $BRAF^{V600E}$ active site, respectively.

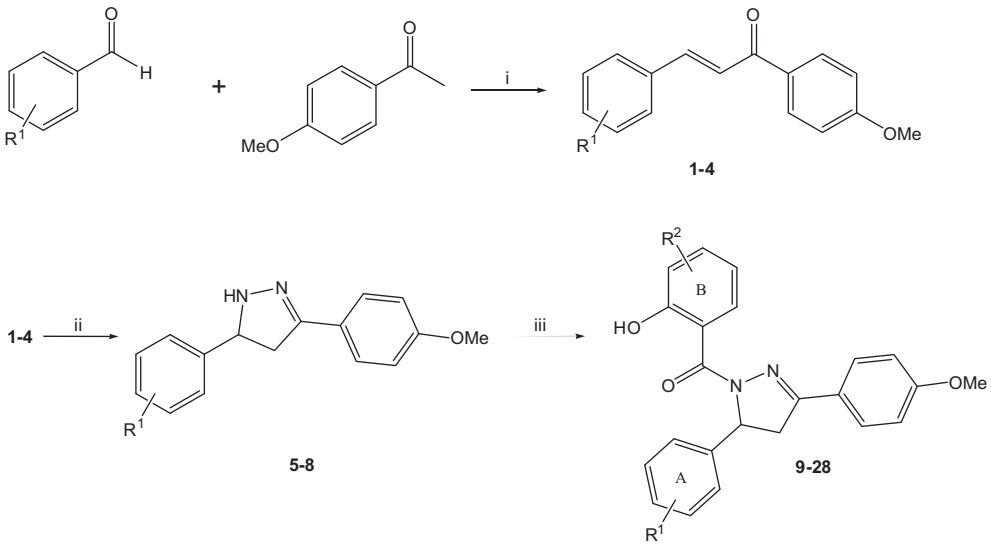

Scheme 1. Synthesis route of 4, 5-dihydro-1*H*-pyrazole salicylamide derivatives **9**–**28**. Reagents and conditions: (i) 40% KOH, ethanol, 5–10 °C, 4 h; R^1 = 4-benzyloxy, 4-OMe, 4-Cl, 4-Br; (ii) $N_2H_4{\cdot}H_2O$, ethanol, reflux, 2 h; (iii) EDC·HCl and HOBt, CH_2Cl_2, reflux, overnight; R^2 = 5-Cl, 4-Cl, 5-Br, 5-I, 5-OMe.

Table 2
$BRAF^{V600E}$ kinase and cellular activity of 4, 5-dihydro-pyrazole salicylamide analogs **9–28**

Compound	R^1	R^2	$BRAF^{V600E}$ IC_{50}, μM	WM266.4 GI_{50}, μM
9	4-Benzyloxy	5-Cl	5.69 ± 0.92	12.9 ± 0.52
10	4-Benzyloxy	4-Cl	5.01 ± 0.75	7.89 ± 0.31
11 (**Hit 1**)	4-Benzyloxy	5-Br	7.22 ± 0.59	12.86 ± 0.97
12	4-Benzyloxy	5-I	5.9 ± 0.31	13.03 ± 0.29
13	4-Benzyloxy	5-OMe	10.34 ± 1.2	13.92 ± 1.1
14	4-OMe	5-Cl	9.3 ± 1.5	12.63 ± 0.64
15	4-OMe	4-Cl	7.04 ± 0.44	13.3 ± 0.5
16	4-OMe	5-Br	4.92 ± 0.61	18.4 ± 1.6
17	4-OMe	5-I	13.3 ± 0.9	15.6 ± 0.78
18 (**Hit 2**)	4-OMe	5-OMe	8.38 ± 0.44	>20
19	4-Br	5-Cl	2.51 ± 0.27	3.48 ± 0.17
20	4-Br	4-Cl	1.38 ± 0.1	2.89 ± 0.56
21	4-Br	5-Br	3.69 ± 0.18	7.4 ± 0.33
22	4-Br	5-I	4.1 ± 0.72	7.35 ± 0.3
23	4-Br	5-OMe	6.94 ± 1.21	12.9 ± 0.82
24	4-Cl	5-Cl	0.57 ± 0.13	1.52 ± 0.5
25	4-Cl	4-Cl	0.16 ± 0.03	0.24 ± 0.07
26	4-Cl	5-Br	1.21 ± 0.09	2.39 ± 0.82
27	4-Cl	5-I	1.30 ± 0.53	3.27 ± 0.13
28	4-Cl	5-OMe	3.72 ± 0.64	5.04 ± 0.6
Sorafenib[a]			0.06	8.1

[a] Used as a positive control.

Table 3
$BRAF^{WT}$ cellular activity, $BRAF^{V600E}$ cell based pERK activity and kinase inhibitory activities against selected kinases of compound **25**

WM1361 (μM)	12.1 ± 0.98
pERK	0.81 ± 0.19
EGFR	10.49 ± 0.5
HER-2	>25
FAK	>25
Aurora-A	>25
IC_{50} VEGFR-2	>25

The inhibitory activities are displayed as IC_{50} (μM).

WM266.4). The protocols of biological assay were described in **part 3** of Supplementary data.

As shown in Table 2, a number of synthesized 3,5-diarylpyrazoline salicylamide analogues displayed potent $BRAF^{V600E}$ kinase inhibitory activities in the low micromolar range. In general, several analogues exhibited good activity with IC_{50} values of less than that of **Hit 1**, two compounds (**24, 25**) demonstrated IC_{50} values of <1 μM. A comparison of the *para* substitution on A ring demonstrated that a *para* halogen group (**19–28**) may have more slightly improved inhibitory activity than a benzyloxy or a methoxy group, and it showed the most potent inhibitory activity when the *para* position substituted by chlorine (**24–28**). The inhibitory activity of compounds with different para substituents on B ring increased in the following order: 4-methoxy < 4-benzyloxy < 4-Br < 4-Cl. The result suggested that strongly electronic-withdrawing substituents on phenyl B ring were beneficial for the activity. SAR also indicated that compounds bearing the same substituent on phenyl A ring exhibited distinct kinase inhibitory activity due to different substituents which introduced into salicylic B ring. Introduction of groups with greater electronegativity results in more active analogs. The fact that the stronger electron-withdrawing substituents at 5-position on B ring, the more potent it showed, was illustrated by the potency order methoxy < I < Br < Cl. Most significantly, move of Cl substituent to 4-position of salicylic B ring results in the most active analog (**25**) in the whole series. Compound **25** exhibited the most potent inhibitory activity in $BRAF^{V600E}$ kinase inhibition (IC_{50} = 0.16 μM), being exactly comparable to the positive control (Sorafenib).

As described above, the V600E mutant BRAF protein-kinase was considered as an important target for the development of small molecule inhibitors in the treatment human melanoma. Then **9–28** were evaluated for antiproliferative activities against WM266.4 human melanoma cell line expressing V600E mutant BRAF. As illustrated in Table 2, most of the compounds displayed GI_{50} in the low micromolar range. We observed that these compounds, which have potent $BRAF^{V600E}$ kinase inhibitory activities, displayed corresponding optimal cytotoxic activities against mutant BRAF-dependent WM266.4 cells. These results indicated that these compounds were potential anti-melanoma agents for

Table 4
Experimental, predicted inhibitory activity of compounds **9–28** by 3D-QSAR models based upon active conformation achieved by molecular docking

Compound[a]	$BRAF^{V600E}$		Residual error
	Actual pIC_{50}	Predicted pIC_{50}	
9	5.24489	4.93531	0.30958
10	5.30016	5.21236	0.0878
11	5.14146	4.90011	0.24135
12	5.22915	5.05946	0.16969
13	4.98548	4.92129	0.06419
14	5.03152	5.06312	−0.0316
15	5.15243	5.49426	−0.34183
16	5.3078	5.43737	−0.12957
17	4.87615	4.90588	−0.02973
18	5.07654	5.22072	−0.14418
19	5.60033	5.75179	−0.15146
20	5.86012	5.82435	0.03577
21	5.43297	5.58784	−0.15487
22	5.38722	5.62821	−0.24099
23	5.15864	5.38962	−0.23098
24	6.24413	5.99389	0.25024
25	6.79588	6.31049	0.48539
26	5.91721	5.77	0.14721
27	5.88606	5.74181	0.14425
28	5.42946	5.86954	−0.44008

[a] Underlined compounds were selected as the test sets while the rest ones were in the training sets.

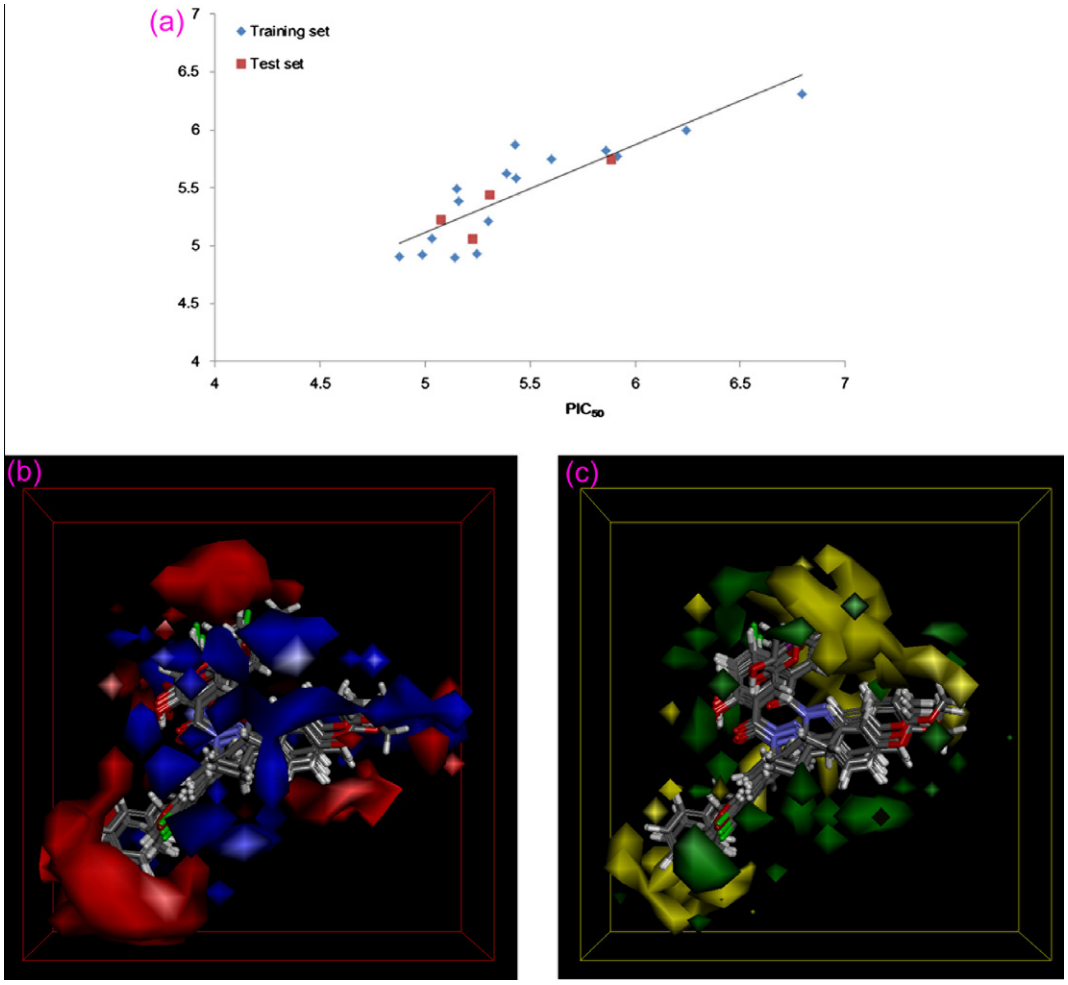

Figure 2. (a) The predicted versus experimental pIC_{50} value for the inhibition of $BRAF^{V600E}$; (b) Isosurface of the 3D-QSAR model coefficients on electrostatic potential grids with positive electrostatic potential in blue triangle mesh representation and the negative in red area for the aligned molecular structures. (c) Isosurface of the 3D-QSAR model coefficients on Van der Waals grids. The green triangle mesh representation indicates positive coefficients; the yellow triangle mesh indicates negative coefficients.

inhibiting mutant BRAF, and further validated that V600E mutant BRAF was an effective target for melanoma therapy.

For the sake of assess the inhibition of the target signaling pathway (RAF-ERK) by compound **25**, the phosphorylation level of extracellular signal-regulated kinase (ERK) was measured in a cell-based assay (IC_{50} pERK). As shown in Table 3, compound **25** exhibited obviously inhibitory activity of ERK phosphorylation in BRAF mutant cell line. Furthermore, in order to provide evidence to the specificity of the compounds in inhibition of mutant BRAF-driven cell proliferation, the antiproliferative activities for the BRAF wild-type WM1361 melanoma cell line (GI_{50} WM1361) that did not express mutant BRAF was determined for compound **25** which had the most potent $BRAF^{V600E}$ inhibitory activity and the result were exhibited in Table 3. Compared to the GI_{50} values on mutant BRAF melanoma cell line WM266.4, the obtained GI_{50} WM1361 of these inhibitors was up to dozens of times. These positive results strongly support compound **25** possess antiproliferative activities against BRAF melanoma cell line through the selective inhibition of oncogenic BRAF. To probe the kinase selectivity of compound **25** against BRAF over other kinases, we selected five kinases, EGFR, HER-2, FAK, Aurora-A, and VEGFR-2 which validated as key regulators in cell cycle. The results revealed that the compound has an excellent selectivity profile. As shown in Table 3, compound **25** did not show significant inhibitory activities against HER-2, FAK, Aurora-A, and VEGFR-2, and it showed EGFR inhibition with an IC_{50} value of more than 10 μM. Taken together, our data establish compound **25** as a potent and selective $BRAF^{V600E}$ inhibitor.

Based on the binding models, the 3D-QSAR (Quantitative Structure–Activity Relationship) modeling was performed to give further validation of the binding mode and provided a structural framework for understanding the structure–activity relationship of these compounds. The 3D-QSAR models were built using the corresponding pIC_{50} ($-\log IC_{50}$) values which were transformed from obtained $BRAF^{V600E}$ IC_{50} (in Mol/L) and performed by QSAR software of DS 3.1 (Discovery Studio 3.1, Accelrys, Inc., San Diego, CA). The training and test set was chosen by the Diverse Molecules method in DS 3.1. The training sets were composed of 16 inhibitors and test sets comprised 4 compounds of data sets as list in Table 4. The underlined compounds in Table 4 were selected into test sets and the rest were in training sets. One of the important steps in developing 3D-QSAR modeling is the determination of active conformation and alignment of molecules. An efficient solution in this study is to depend on docking programs and the reliability of this method has been documented in previous studies.[22,24] The alignment conformation of each molecule was the one with lowest energy in the docked results of CDOCKER.

The 3D-QSAR model generated from DS 3.1, defines the critical regions (steric or electrostatic) affecting the binding affinity. It was a PLS model built on 400 independent variables (conventional

r^2 = 0.754). The observed and predicted values and their residual values for the training set and test set molecules in 3D-QSAR model are given in Table 4 and their graphical relationship is illustrated in Figure 2A, respectively. The plot of the observed IC_{50} vs. the predicted results shows that this model has a good predictive power which can be used in prediction of activity for new pyrazole salicylamide derivatives as $BRAF^{V600E}$ inhibitors.

A contour plot of the electrostatic field region favorable (in blue) or unfavorable (red) for the $BRAF^{V600E}$ affinity is shown in Figure 2B. The energy grids corresponding to the favorable (in green) or unfavorable (yellow) steric effects for the $BRAF^{V600E}$ affinity are shown in Figure 2C. A good ligand should have strong Van der Waals attraction in the green areas and a polar group in the blue electrostatic potential areas (which are dominant close to the skeleton). Several key features of the 3D-QSAR contour map are predicted to increase $BRAF^{V600E}$ affinity: (1) More bulk near the phenolic hydroxyl group and less bulk 5-substituent group of ring B (steric study); (2) More bulk group substituted in the *ortho* and *meta* position of ring A (steric study); (3) A more positive environment all around the *para* position of the 4-methoxyphenyl ring and ring B (electronic study); (4) A more negative environment around the *ortho* position of ring B (electronic study).

In conclusion, virtual screening of our designed pyrazole derivatives resulted in the identification of 3,5-diarylpyrazoline salicylamide derivative **Hit 1**, which served as the starting point for the design of potent V600E mutant BRAF inhibitors. In order to obtain more pharmacophore understandings of 4, 5-dihydro-pyrazole salicylamide derivatives as $BRAF^{V600E}$ inhibitors and rational structural optimization, a series of novel analogues of **Hit 1** have been designed and prepared. Compound **25** displayed the most potent inhibitory activity, with IC_{50} value of 0.16 μM for $BRAF^{V600E}$ and GI_{50} value of 0.24 μM for mutant BRAF-dependent WM266.4 cells. The $BRAF^{WT}$ cellular activity and $BRAF^{V600E}$ cell based pERK activity of compound **25** suggested it could selectively inhibit proliferation of mutant BRAF-dependent melanoma cell line through inhibition of oncogenic BRAF. The SAR analysis was performed to provide crucial pharmacophore clues that could use in further structure optimization. Above all, the results obtained from this study suggest that 3,5-diarylpyrazoline salicylamide skeleton may serve as a novel scaffold for the further development of more potent and selective $BRAF^{V600E}$ inhibitors which use as mutant BRAF-dependent melanoma therapeutic agents.

Acknowledgment

This work was financed by National Natural Science Foundation of China (No. J1103512).

Supplementary data

Supplementary data associated with this article can be found, in the online version, at http://dx.doi.org/10.1016/j.bmcl.2012.09.004.

References and notes

1. Robinson, M. J.; Cobb, M. H. *Curr. Opin. Cell Biol.* **1997**, *9*, 180.
2. Johnson, G. L.; Lapadat, R. *Science* **1911**, *2002*, 298.
3. Friday, B. B.; Adjei, A. A. *Clin. Cancer Res.* **2008**, *14*, 342.
4. Kyriakis, J. M.; Avruch, J. *Physiol. Rev.* **2001**, *81*, 807.
5. Wellbrock, C.; Karasarides, M.; Marais, R. *Nat. Rev. Mol. Cell Biol.* **2004**, *5*, 875.
6. Avruch, J.; Khokhlatchev, A.; Kyriakis, J. M.; Luo, Z.; Tzivion, G.; Vavvas, D.; Zhang, X. F. *Recent Prog. Horm. Res.* **2001**, *56*, 127.
7. Davies, H.; Bignell, G. R.; Cox, C.; Stephens, P.; Edkins, S.; Clegg, S.; Teague, J.; Woffendin, H.; Garnett, M. J.; Bottomley, W.; Davis, N.; Dicks, E.; Ewing, R.; Floyd, Y.; Gray, K.; Hall, S.; Hawes, R.; Hughes, J.; Kosmidou, V.; Menzies, A.; Mould, C.; Parker, A.; Stevens, C.; Watt, S.; Hooper, S.; Wilson, R.; Jayatilake, H.; Gusterson, B. A.; Cooper, C.; Shipley, J.; Hargrave, D.; Pritchard-Jones, K.; Maitland, N.; Chenevix-Trench, G.; Riggins, G. J.; Bigner, D. D.; Palmieri, G.; Cossu, A.; Flanagan, A.; Nicholson, A.; Ho, J. W.; Leung, S. Y.; Yuen, S. T.; Weber, B. L.; Seigler, H. F.; Darrow, T. L.; Paterson, H.; Marais, R.; Marshall, C. J.; Wooster, R.; Stratton, M. R.; Futreal, P. A. *Nature* **2002**, *417*, 949.
8. Garnett, M. J.; Marais, R. *Cancer Cell* **2004**, *6*, 313.
9. Tuveson, D. A.; Weber, B. L.; Herlyn, M. *Cancer Cell* **2003**, *4*, 95.
10. Wan, P. T. C.; Garnett, M. J.; Roe, S. M.; Lee, S.; Niculescu-Duvaz, D.; Good, V. M.; Jones, C. M.; Marshall, C. J.; Springer, C. J.; Barford, D.; Marais, R. *Cell* **2004**, *116*, 855.
11. Hingorani, S. R.; Jacobetz, M. A.; Robertson, G. P.; Herlyn, M.; Tuveson, D. A. *Cancer Res.* **2003**, *63*, 5198.
12. Karasarides, M.; Chiloeches, A.; Hayward, R.; Niculescu-Duvaz, D.; Scanlon, I.; Friedlos, F.; Ogilvie, L.; Hedley, D.; Martin, J.; Marshall, C. J.; Springer, C. J.; Marais, R. *Oncogene* **2004**, *23*, 6292.
13. Gould, A. E.; Adams, R.; Adhikari, S.; Aertgeerts, K.; Afroze, R.; Blackburn, C.; Calderwood, E. F.; Chau, R.; Chouitar, J.; Duffey, M. O.; England, D. B.; Farrer, C.; Forsyth, N.; Garcia, K.; Gaulin, J.; Greenspan, P. D.; Guo, R.; Harrison, S. J.; Huang, S. C.; Iartchouk, N.; Janowick, D.; Kim, M. S.; Kulkarni, B.; Langston, S. P.; Liu, J. X.; Ma, L. T.; Menon, S.; Mizutani, H.; Paske, E.; Renou, C. C.; Rezaei, M.; Rowland, R. S.; Sintchak, M. D.; Smith, M. D.; Stroud, S. G.; Tregay, M.; Tian, Y.; Veiby, O. P.; Vos, T. J.; Vyskocil, S.; Williams, J.; Xu, T.; Yang, J. J.; Yano, J.; Zeng, H.; Zhang, D. M.; Zhang, Q.; Galvin, K. M. *J. Med. Chem.* **1836**, *2011*, 54.
14. Bollag, G.; Hirth, P.; Tsai, J.; Zhang, J. Z.; Ibrahim, P. N.; Cho, H. N.; Spevak, W.; Zhang, C.; Zhang, Y.; Habets, G.; Burton, E.; Wong, B.; Tsang, G.; West, B. L.; Powell, B.; Shellooe, R.; Marimuthu, A.; Nguyen, H.; Zhang, K. Y. J.; Artis, D. R.; Schlessinger, J.; Su, F.; Higgins, B.; Iyer, R.; D'Andrea, K.; Koehler, A.; Stumm, M.; Lin, P. S.; Lee, R. J.; Grippo, J.; Puzanov, I.; Kim, K. B.; Ribas, A.; McArthur, G. A.; Sosman, J. A.; Chapman, P. B.; Flaherty, K. T.; Xu, X. W.; Nathanson, K. L.; Nolop, K. *Nature* **2010**, *467*, 596.
15. Wellbrock, C.; Hurlstone, A. *Biochem. Pharmacol.* **2010**, *80*, 561.
16. Barsoum, F. F.; Hosni, H. M.; Girgis, A. S. *Bioorg. Med. Chem.* **2006**, *14*, 3929.
17. Ghorab, M. M.; Ragab, F. A.; Alqasoumi, S. I.; Alafeefy, A. M.; Aboulmagd, S. A. *Eur. J. Med. Chem.* **2010**, *45*, 171.
18. Liu, X. H.; Cui, P.; Song, B. A.; Bhadury, P. S.; Zhu, H. L.; Wang, S. F. *Bioorg. Med. Chem.* **2008**, *16*, 4075.
19. Luo, C.; Xie, P.; Marmorstein, R. *J. Med. Chem.* **2008**, *51*, 6121.
20. Kim, M. H.; Kim, M.; Yu, H.; Kim, H.; Yoo, K. H.; Sim, T.; Hah, J. M. *Bioorg. Med. Chem.* **1915**, *2011*, 19.
21. Discovery Studio 3.1, Accelrys Software Inc., San Diego, 2011.
22. Wu, G.; Robertson, D. H.; Brooks, C. L.; Vieth, M. *J. Comput. Chem.* **2003**, *24*, 1549.
23. King, A. J.; Patrick, D. R.; Batorsky, R. S.; Ho, M. L.; Do, H. T.; Zhang, S. Y.; Kumar, R.; Rusnak, D. W.; Takle, A. K.; Wilson, D. M.; Hugger, E.; Wang, L. F.; Karreth, F.; Lougheed, J. C.; Lee, J.; Chau, D.; Stout, T. J.; May, E. W.; Rominger, C. M.; Schaber, M. D.; Luo, L. S.; Lakdawala, A. S.; Adams, J. L.; Contractor, R. G.; Smalley, K. S. M.; Herlyn, M.; Morrissey, M. M.; Tuveson, D. A.; Huang, P. S. *Cancer Res.* **2006**, *66*, 11100.
24. Dai, Y.; Wang, Q.; Zhang, X.; Jia, S.; Zheng, H.; Feng, D.; Yu, P. *Eur. J. Med. Chem.* **2010**, *45*, 5612.